



This item was submitted to Loughborough's Institutional Repository (<https://dspace.lboro.ac.uk/>) by the author and is made available under the following Creative Commons Licence conditions.



CC creative commons
COMMONS DEED

Attribution-NonCommercial-NoDerivs 2.5

You are free:

- to copy, distribute, display, and perform the work

Under the following conditions:

BY: **Attribution.** You must attribute the work in the manner specified by the author or licensor.

Noncommercial. You may not use this work for commercial purposes.

No Derivative Works. You may not alter, transform, or build upon this work.

- For any reuse or distribution, you must make clear to others the license terms of this work.
- Any of these conditions can be waived if you get permission from the copyright holder.

Your fair use and other rights are in no way affected by the above.

This is a human-readable summary of the [Legal Code \(the full license\)](#).

[Disclaimer](#) 

For the full text of this licence, please go to:
<http://creativecommons.org/licenses/by-nc-nd/2.5/>

Application of fault detection and isolation to a pneumatic actuation system

K.S.Grewal^{*}, R. Dixon^{*}, J. Pearson^{**}

^{*} *Control Systems Group, Loughborough University, Loughborough, Leicestershire, UK.*

^{**} *SEIC, BAE Systems, Holywell Park, Loughborough, Leicestershire, UK.*

Abstract: This paper discusses research carried-out on the development and validation (on real plant) of a parity-equation based fault detection and isolation (FDI) system for a pneumatic actuator. A mechanistic model of the system is developed and validated in order to derive suitable parity equations for the pneumatic actuation system. The parity equations are then formulated and used to generate residuals that, in turn, are analysed to determine whether faults are present in the system. Details of the design process are given and the experimental results demonstrate that the approach can successfully detect and isolate faults associated with the sensors, actuators (servo-valves and piping) and the pneumatic cylinder itself. The work is part of a BAE SYSTEMS' sponsored project to demonstrate advanced control and diagnosis concepts on a Stewart-Gough platform.

Keywords: Fault detection; isolation; residuals; modeling; pneumatic; parity equations

1. INTRODUCTION

The design of schemes for the detection and diagnosis of faults is becoming increasingly important in engineering due to the complexity of modern industrial systems and growing demands for quality, cost efficiency, reliability, and more importantly the safety issue (Al-Najjar, 1996). In industrial plant, early detection of developing faults can allow planned maintenance work to take place before a system malfunctions, possibly causing damage, or complete shut-down of the system/plant. This improves the level of plant safety, and increases the plant availability and profitability. In safety/mission critical applications, fault detection can be combined with reconfiguration (after a fault) to achieve fault tolerant control - allowing the system to complete its function in a way that is sub-optimal but does achieve the design objective.

There two principal approaches to detection and isolation of faults:

- Hardware redundancy - this involves comparing the outputs of identical hardware (sensors/actuators) and performing consistency cross-checks.
- Analytical redundancy – combining sensor signals, control signals and models to arrive at estimates of unmeasured/immeasurable variables.

Model-based Fault Detection and Isolation (FDI) uses the principles of analytical redundancy to first *detect* deviations from normal behaviour in a system, and then to *isolate* the particular component that has a fault. Typically, model-based analytical estimates are compared with measured variables to generate residuals. The residuals will be zero when the system is operating normally and will be non-zero when a fault arises. There are a number of approaches to model-based residual generation. For example, observer-based approaches including Kalman Filters (Frank, 1990), parity

relations approaches (Gertler and Singer, 1990) and parameter estimation (Patton *et al* 2000), Isermann, (1997). Useful surveys of these and other useful FDI methods can be found in Patton (1997), Iserman (1984), Willsky (1976), and Venkatasubramaniam *et al* (2003). However, most of the fault tolerant literature available deals with systems in a purely theoretical way or uses simulations to demonstrate the methods. Although many of the concepts work well in theory, it is clear that there have been limited real industrial applications particularly of the more advanced techniques.



Fig. 1. Single pneumatic actuator test-rig

The work described in this paper is part of an on going project which aims to demonstrate FDI as part of a fault tolerant control system on a Stewart-Gough platform comprising six pneumatic actuators. The first phase of the work has focussed on modelling, control and FDI applied to a single actuator (see figure 1).

This paper reports results obtained from experiments on the rig using the parity equation approach to FDI. The paper is organised as follows, in section 2 the experimental set-up is

described; section 3 summarises the mathematical model of the pneumatic system (including validation results), which is used as the foundation of the control and FDI design; section 4 describes the FDI approach and how the parity equations are applied to the pneumatic system; section 5 presents and discusses the results for the four different fault cases; finally, conclusions are drawn and future work is discussed in section 6.

2. EXPERIMENTAL SET-UP

The experimental set-up is illustrated in Figure 2. The set-up shows the xPC Target coupled with Matlab/Simulink®, which provides a real-time environment. A host and a target computer are connected using a TCP/IP network. Matlab/Simulink® is run on the host computer, this is where the control and FDI system is designed using xPC target I/O blocks. Using external mode the system file is built and compiled within the host computer. Then downloaded to the target computer where it is executed using the real-time kernel. The position signal is measured via a Linear Resistive Transducer (LRT) mounted in the cylinder rear section. The acceleration signal is acquired using an accelerometer mounted on the end of the piston rod.

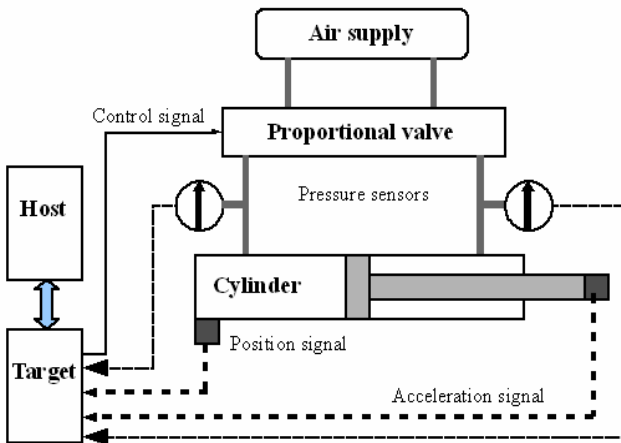


Fig. 2. Schematic of experimental set-up

3. MODELLING OF PNEUMATIC SYSTEM

An early attempt to analyse pneumatic control systems was reported by Shearer (1956). This was further extended by Burrows (1969), and Scavarda *et al* (1987). One of the main problems in pneumatic actuator position control is the highly non-linear equations that model the system. This means that classical linear controller synthesis methods difficult to apply. Moreover, due to the non-linearity, the parameters of these equations are usually very difficult to identify. However, using approximation of the model, allows the use of a restricted range of the optimum parameters that are selected with classical methods (Chillari *et al*, 2001). For a detailed description of the mathematical model of the pneumatic system see Grewal *et al* (2008). The pneumatic circuit to be modelled is depicted in Figure 3.

3.1. Pneumatic Model

The relationship between the air mass flow and the pressure

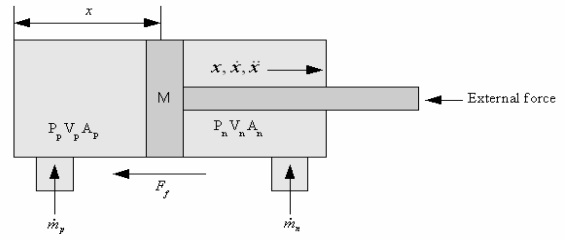


Fig. 3. Schematic of the double acting cylinder.

changes in the chambers is obtained using energy conservation laws (first law of thermodynamics), and the force equilibrium is given by Newton's second law. Where M is the piston mass, A is the bore area, P_p is the pressure in chamber p , P_n is the pressure in chamber n , V_p is the air volume in chamber p , V_n is the air volume in chamber n , T_s is the operating temperature, \dot{m}_p is the mass flow rate into chamber p , and \dot{m}_n is the mass flow rate into chamber n . The relationship between the mass flow rate of air and the change of both pressure and volume in chambers can be written as:

$$\dot{m}_p = \frac{V_p}{\gamma RT_s} \frac{dP_p}{dt} + \frac{P_p}{RT_s} \frac{dV_p}{dt} \quad (1)$$

$$\dot{m}_n = \frac{V_n}{\gamma RT_n} \frac{dP_n}{dt} + \frac{P_n}{RT_s} \frac{dV_n}{dt} \quad (2)$$

Where, γ is the ratio of specific heat, R is the universal gas constant. The dynamics of the cylinder motion can be described by:

$$M\ddot{x} + F_f\dot{x} = A(P_p - P_n) = A\Delta P \quad (3)$$

Where x is the position of the piston, F_f represents the viscous friction coefficient and coulomb friction force. The mass flow rate is identical (in magnitude) for both chambers and is proportional to the valve input voltage (v). Hence

$$\dot{m}_p = Kv \quad \text{and} \quad \dot{m}_n = -Kv \quad (4)$$

Where K is the servo valve constant ($\text{Kg.s}^{-1}.\text{v}^{-1}$) determined from the valve's data-sheet. With the assumption of incompressibility the rate of change of volumes can be written as

$$\dot{V}_p = A\dot{x} \quad \text{and} \quad \dot{V}_n = -A\dot{x} \quad (5)$$

Substituting equation (4) and (5) into equations (1) and (2), then rearranging the equations for chambers p and n gives:

$$\dot{P}_p = -\frac{\gamma AP_p}{V_p} \dot{x} + K \frac{\gamma RT_s}{V_p} v \quad (6)$$

$$\dot{P}_n = \frac{\gamma AP_n}{V_n} \dot{x} - K \frac{\gamma RT_s}{V_n} v \quad (7)$$

Then rearranging equation (3) gives:

$$\ddot{x} = \frac{A}{M} (P_p - P_n) - \frac{F_f}{M} \dot{x} \quad (8)$$

The overall model makes use of equations (6), (7), and (8) implemented either in state-space or block diagram form (in, e.g. Matlab/Simulink).

3.2. Model validation

In order to validate the model a number of experiments were carried out on the open-loop actuator and the results compared with those from simulation. A typical set of results for a square wave input is shown in Figure 4. Here, the square wave input is set at 0.6 volts and the frequency set at 0.5Hz, and the position and the pressure output responses are plotted alongside those predicted by the model. The periodic step input is used because a step has all frequencies of interest present (so should excite all the key dynamics). The simulation results show reasonable agreement with those from the experiment. The position results show a particularly good match, whilst those for the two cylinders pressures capture the dominant response, though there is clearly some longer-term mode that is not represented in the model. These differences are thought to be due to non-linearities associated with pneumatic systems that are not captured in the model.

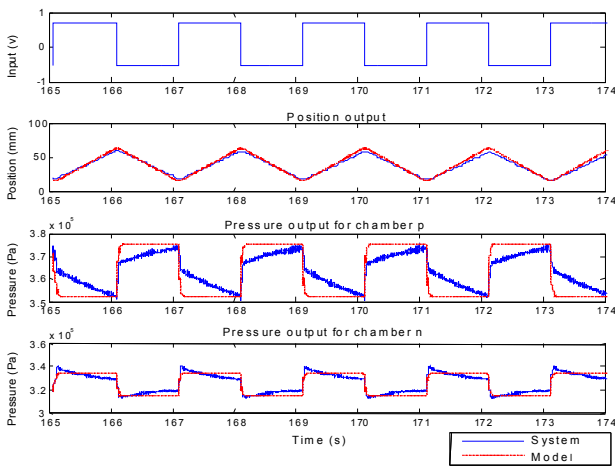


Fig. 4. The comparisons between the system and model outputs for a square wave input.

4. DESIGN OF THE FDI SCHEME

4.1 FDI Approach

Figure 5 shows the generic structure of the model-based fault detection scheme. The method consists of detecting faults on the process, which includes actuators, components and sensors, based on measuring the input signal $U(t)$ and the output signal $Y(t)$. The detection method uses models to generate residuals $R(t)$. The residual evaluation examines the residuals for the likelihood of faults and a decision rule is applied to determine if faults have occurred. Referring to the pneumatic system depicted in Figure 1 (and with reference to Figure 5) the proportional valve would be described as the actuator and the pneumatic cylinder would be described as the plant. The sensors are self-evident.

4.2. The Parity Equation Method

The parity equation method was proposed by Chow and Willsky, (1984) using the redundancy relations of the dynamic system. The basic idea is to provide a proper check of the parity (consistency) of the measurements for the

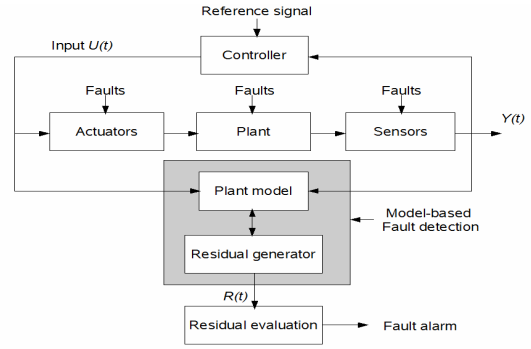


Fig. 5. Conceptual structure of FDI scheme

monitored system. Parity equations are rearranged and usually transformed variants of the input-output or space-state models of the system (Venkatasubramaniam *et al* 2003). In effect this means making use of known mathematical models that describe the relationships between system variables. In theory, under normal operating conditions, the residual or value of the parity equations is zero. However, in real situations the residuals will be nonzero. This is due to measurement and process noise, model inaccuracies, errors in sensors and actuators, including faults in plants. The idea of the parity approach is to rearrange the model structure to achieve the best fault isolation (i.e. so that the effect of faults is far greater than that of the other uncertainties). The residual generator scheme used hereafter is based on a classical model-based methodology using the parity space approach. The desired properties for the residual signal $r(t)$ are $r(t) \neq 0$ if $f, f(t) \neq 0$. Where r is the residual and f is the fault. The residual is generated based on the information provided by the system input and output signals using a residual generation (Patton and Chen, 1997). Figure 6 shows the pneumatic control loop scheme, which contains the following elements: The controller $C(s)$, the proportional valve $GA(s)$, the pneumatic actuator $GP(s)$, and the sensor $GS(s)$.

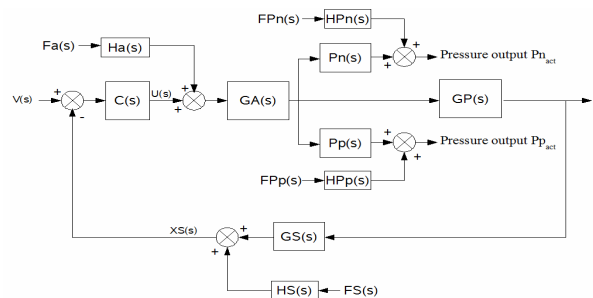


Fig. 6. Pneumatic closed loop scheme with additive faults

The actuator fault $Fa(s)$ and the sensor fault $FS(s)$ can have dynamics which are modelled by the transfer functions $Ha(s)$, and $HS(s)$. In addition to the position (feedback) sensor, pressure sensors are included in the system to read pressure from each chamber of the actuator. These are not included in the closed loop control system, but may be used for fault detection, and are shown as $Pp(s)$ and $Pn(s)$ respectively. With the pressure sensor faults shown as $FPP(s)$ and $FPn(s)$. The pressure sensor faults are modelled by the transfer

functions $HPp(s)$ and $HPn(s)$. Using the description of the system shown in Figure 6 the following relationships can be derived. This method of parity equations is taken from Biacheche *et al* (1994).

$$XS(s)=[GS(s)+HS(s)FS(s)][GP(s)GA(s)U(s)+Ha(s)Fa(s)] \quad (9)$$

$$Pn_{act}=[U(s)GP(s)+Ha(s)Fa(s)][Pn(s)+HPn(s)FPn(s)] \quad (10)$$

$$Pp_{act}=[U(s)GP(s)+Ha(s)Fa(s)][Pp(s)+HPp(s)FPp(s)] \quad (11)$$

$$U(s)=C(s)(V(s)-XS(s)) \quad (12)$$

Equation (12) is an analytical redundancy relation and implies the assumption that all signals are available for measurement. However, in reality for an industrial application the controller signal $U(s)$ is not usually measured. Using equations (9) to (12) the following residuals can be formulated:

$$R_1=XS(s)-GS(s)GP(s)GA(s)U(s)=HS(s)FS(s)+HaFa(s) \quad (14)$$

$$R_2= Pn_{act} - U(s)GA(s)Pn(s)=Ha(s)Fa(s)+HPn(s)FPn(s) \quad (15)$$

$$R_3= Pp_{act} - U(s)GA(s)Pp(s)=Ha(s)Fa(s)+HPp(s)FPp(s) \quad (16)$$

4.3. Residual Evaluation and Thresholds

The purpose of residual evaluation is to generate a fault decision by processing the residuals. A fault decision is the result of all the tasks fault detection, isolation, and identification (Kiencke and Nielsen, 2005). Residual evaluation is essentially to check if the residual is responding to a fault. The residual evaluation can in its simplest form be a thresholding of the residual, i.e. a fault is assumed present if $|R_i(t)| > J_i(t)$ where $J_i(t)$ is the threshold, or moving averages of the residuals. Another method may consist of statistical sequential probability ratio testing (Patton *et al*, 2000). In the present case the residuals are processed to acquire the root mean square (RMS) of the value over a moving window of N samples (Dixon, 2004) as shown:

$$R_{i,RMS}(k) = \sqrt{\frac{\sum_{j=k-N}^k R_{ij}^2}{N}} \quad i = 1, 2, 3 \quad (18)$$

Where $R_i(k)$ is the value of the residual at the k_{th} sample. Subsequently, the residual RMS value is compared with a predetermined fault detection threshold. The thresholds for the system have been set such that if the fault applied causes a decrease in performance of 20% then a fault flag is fired. Table 1 shows the fault signatures of the pneumatic system for different single faults. These are identified by inspection from Figure 6 and the combination of faults flags can be used to isolate faults.

5. EXPERIMENTAL RESULTS

In order to demonstrate the FDI scheme using parity equations a number of experiments were carried out on the pneumatic system (Figures 1 and 2). The considered faults

Table 1. Fault signatures with additive faults

Residual	Actuator	Pressure sensor Pn	Pressure sensor Pp	Position sensor
R ₁	1	0	0	1
R ₂	1	1	0	0
R ₃	1	0	1	0

for this study are nonparametric faults or additive faults and a drift fault. These are unknown inputs acting on the plant. The occurrence of a fault is modelled by a nonzero output. This affect causes a change in the plant outputs independent of the known inputs. The pneumatic process $GA(s)$ and $GP(s)$ is modelled by the equations (6), (7) and (8). The sensor dynamics are assumed to be instantaneous i.e. $Ha(s)$, $HS(s)$, $HPn(s)$, $HPp(s)$, $Pn(s)$, $Pp(s)$, and $GS(s) = 1$. The system is operated under position control with a PI controller designed to give appropriate closed-loop performance. The fault scenarios considered are summarized in Table 2.

Table 2. Fault characteristics

Test	Fault	Time of appearance	Duration	Magnitude
1	Actuator $Fa(s)$	30 sec	0.5 sec	-5v
2	Pressure sensor $FPn(s)$	25 sec	2.5 sec	-0.5bar
3	Pressure sensor $FPp(s)$	20 sec	2.5 sec	-0.5bar
4	Position sensor $FS(s)$	17 sec	10 sec	2 (slope)

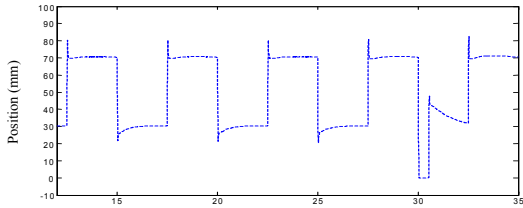
5.1. Actuator fault

An additive fault $Fa(s)$ (see Fig.6) is applied to the proportional valve. A step reduction on $Fa(s)$ simulates a fault in the proportional control valve. This could be due to a fault in the power supply, amplifier or the connection between the control signal and the valve. Figure 8 shows the time history of this experiment. Where plot (8a) shows the actual system output (with fault); plots 8b, 8c, and 8d show the RMS values of the actuator residuals R_1 , R_2 , and R_3 respectively. The state of the actuator fault flag is shown in the lower plot (8e). At 30s the fault occurs, for a period of 0.5s then clears. The fault is detected within 0.5ms. The fault flag is fired within 1.5ms and remains fired until the fault is removed from the system and subsequently, at 30.86s the fault flag returns to the false state when the RMS value falls below the threshold. These results concur with the fault signatures detailed in Table 1.

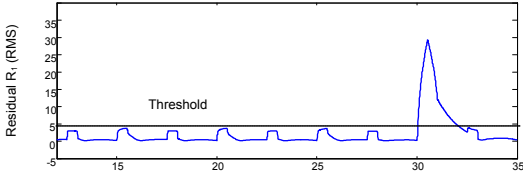
5.2. Pressure sensor (Pn) fault

For an additive fault (FPn) applied to the pressure sensor of chamber n . Figure 9 shows the time history of this experiment. The applied fault emulates that there is a decrease of pressure in the pressure signal from the sensor; in practice this could be due to a faulty connection or a faulty sensor. The upper plot shows the actual pressure sensor output (with fault); the middle plot shows the state of the plant fault flag; and the RMS value of the pressure sensor residual R_2 is shown in the lower plot. At 25s the fault occurs, for a period of 2.5s then clears. The fault is detected within

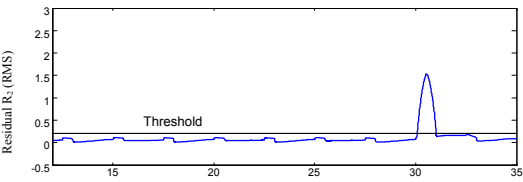
0.5 ms. The fault flag is fired within 1.5ms and remains fired until the fault is removed from the system and subsequently, at 27.65s the fault flag returns to the false state when the RMS value falls below the threshold.



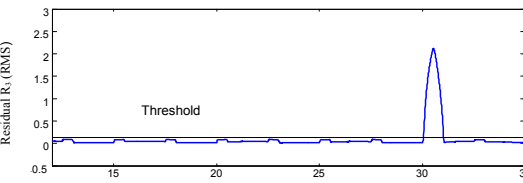
(8a)



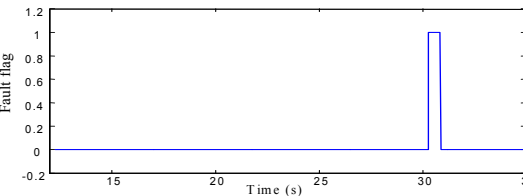
(8b)



(8c)



(8d)



(8e)

Fig. 8. Actuator fault F_a (s) results- actual plant output (8a), the residual evaluation function outputs (8b, 8c, and 8d), actuator fault flag (8e)

5.3. Pressure sensor (P_p) fault

Figure 10 shows the time history of this experiment for an additive fault (F_{Pp}) applied to the pressure sensor of chamber n . The applied fault emulates there is a decrease of pressure in the pressure signal (faulty sensor). The upper plot shows the actual pressure sensor output (with fault); the middle plot shows the state of the plant fault flag; and the RMS value of the pressure sensor residual R_3 is shown in the lower plot. At 20s the fault occurs, for a period of 2.5s then clears. The fault is detected within 0.5ms. The fault flag is fired within 1.5ms and remains fired until the fault is removed from the system and subsequently, at 22.65s the fault flag returns to the false state when the RMS value falls below the threshold.

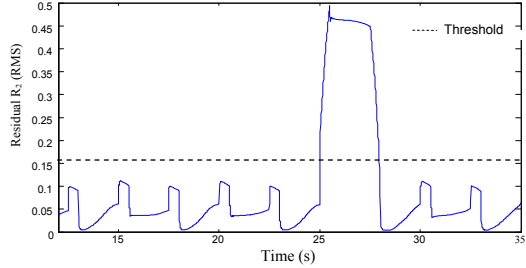
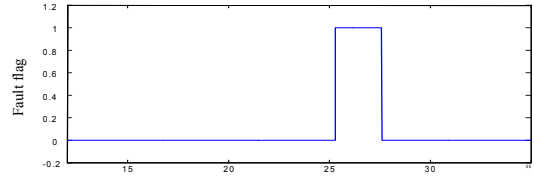
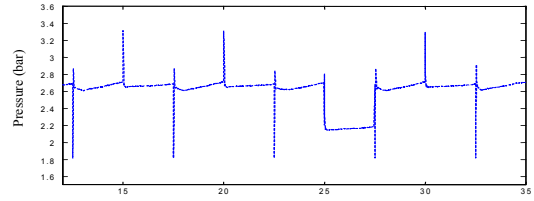


Fig. 9. Pressure sensor P_n fault F_{Pn} (s) results- showing time history of pressure sensor output (top), sensor fault flag (middle), the residual evaluation function output (lower)

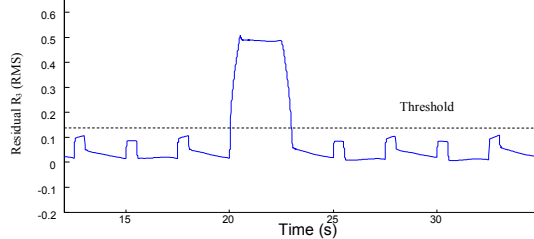
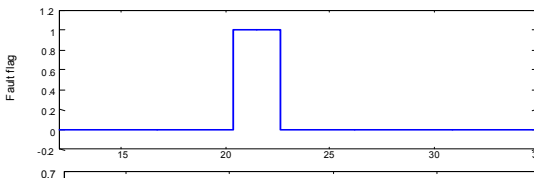
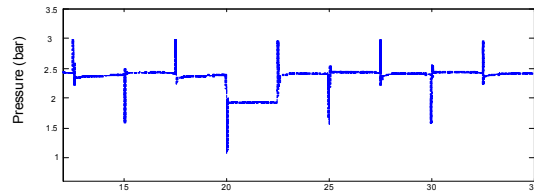


Fig. 10. Pressure sensor P_p fault F_{Pp} (s) results- showing time history of pressure sensor output (top), sensor fault flag (middle), the residual evaluation function output (lower).

5.4. Position sensor (G_S) drift fault

Harsh working conditions along with the gradual build up of dirt on the sensor and faulty circuitry can cause the effect of sensor output drift. From Figure 11, at 17s a drift bias (F_S) is added to the position signal. Although sensor drift can be a slow process i.e. possibly over a period of hours, for this work adding a drift bias within a period of approximately 10s has accelerated the effect of sensor drift. This is so the fault

can be detected and isolated without running the experiment for long periods. From the RMS residual R_1 the drift fault is detected at 17.5s and the fault flag is raised within 0.6ms. The RMS residuals R_2 and R_3 do not activate/cross their respective thresholds. Again, these results concur with the fault signatures detailed in Table 1.

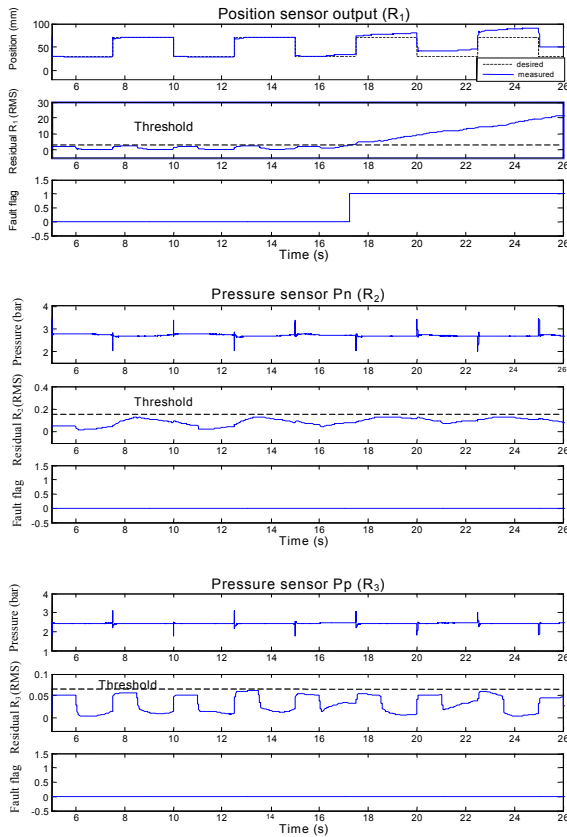


Fig. 11. Position sensor fault - actual plant output-position sensor R_1 (top), Pressure sensor (Pn) R_2 (middle), Pressure sensor (Pp) R_3 (lower)

6. CONCLUSIONS

The paper has described application of a parity equation approach to fault detection in a closed loop pneumatic positioning system. The pneumatic system model has been formulated and typical validation results have been presented. Parity equations have been used to generate residuals and these have been compared to suitable thresholds in order to check the parity (consistency) of the measurements for the monitored system. Nonparametric (additive) faults have been assumed in formulating the equations and have then been applied experimentally to test the efficacy of the detection system.

The results show that, using the described parity equation method, fault detection was possible from the available measurements. Faults in the actuator can be isolated along with the various sensor faults, with position and pressure sensor faults being successfully detected. The test results agree with the fault signatures detailed in Table 1.

An important reason for selecting the parity equation residual generation method was the relative simplicity of the layout

and application of the model equations. It has been shown that despite this simplicity the approach can be used effectively for a real plant with non-linear behaviour. Future work will be focussed on other model-based residual generation schemes.

REFERENCES

- Al-Najjar, B. (1996). Total quality maintenance: An approach for continuous reduction in costs of quality products. *Journal of Quality in Maintenance Engineering*, **2**, pp. 2-20.
- Baikeche, H., Marx, B., Maquin, D., and Ragot, J. (2006) On parametric and non-parametric fault detection in linear closed-loop systems. *4TH Workshop on Advanced Control and Diagnosis, ACD'2006, Nancy, France*.
- Blanke, M., Izadi-Zamanabadi, R., Bogh, S. A., and Lunau, Z. P. (1997). Fault tolerant control systems- A holistic view, *Journal of Control, Engineering Practice*, **5**, (5), pp. 693-702.
- Burrows, C. R. (1969). Non-linear pneumatic servomechanism. PhD Thesis, University of London, UK.
- Chillari, S., Guccione, S., and Muscato, G. (2001). An experimental comparison between several pneumatic position control methods. *Proceedings of the 40th IEEE conference on Decision and Control*. Florida, USA, pp. 1168- 1173.
- Chow, E. Y., and Willsky, A.S (1984). Analytical redundancy and design of robust failure detection systems. *IEEE Trans. on Aut. Control* **29** (7), 603-614.
- Dixon, R (2004). Observer-based FDIA: application to an electromechanical positioning system. *Control Engineering Practice* **12**, pp. 1113-1125.
- Frank, P. M. (1990). Fault diagnosis in dynamic systems using analytical and knowledge-based redundancy: A survey and some new results. *Automatica*, **26**, pp. 459-474.
- Gertler, J., and Singer, D (1990). A new structural framework for parity equation based failure detection and isolation. *Automatica*, **26**, pp. 381-388.
- Grewal, K. S., Dixon, R., and Pearson, J (2008). Development of a fault tolerant actuation system- modelling and validation. *Actuator 08, 11th international conference on new actuators*, pp, 469-472.
- Isermann, R. (1984). Process fault detection based on modelling and estimation methods- A survey. *Automatica*, **20**, pp. 387-404.
- Isermann, R. (1997). Supervision, Fault-Detection and Fault Diagnosis methods- An Introduction, *Control Engineering Practice*, **5**, (5), pp. 639-652.
- Kiencke, U., and Nielsen, L (2005). *Automotive Control Systems: For Engine, Driveline, and Vehicle*. Springer. USA.
- Patton, R.J (1997). Fault-tolerant control: The 1997 situation. *Proceedings of the third symposium on fault detection, supervision and safety for technical processes (SAFEPROCESS'97)*. **3**, pp, 1029-1052.
- Patton, R.J., Frank, P.M., and Clark, R.N. (2000). *Issues in fault diagnosis of dynamic systems*. Springer Verlag. London
- Scavarda, S., Kellal, A., and Richard, E. (1987). Linearized models for electropneumatic cylinder servo valve system. *Proceedings of the 3rd International conference on Advanced Robotics*. France. pp. 149-160.
- Shearer, J. L. (1956). Study of pneumatic processes in the continuous control of motion with compressed air I and II, *Tran. AMSE*, pp. 233-249.
- Venkatasubramanian, V., Rengaswamy, R., Yin, K., and Kavuri, S.N. (2003). A review of process fault detection and diagnosis. Part I: Quantitative model-based methods. *Computers and Chemical Engineering*, **27**, pp. 293-311.